DOI: 10.1002/ejic.200500742

Hydrothermal Synthesis and Structural Characterization of Two pH-Controlled Cd–Squarate Coordination Frameworks, $[Cd_2(C_4O_4)_{2.5}(H_2O)_4]\cdot(dpaH)\cdot 1.5(H_2O)$ and $[Cd(C_4O_4)(dpa)(OH_2)]$ (dpa = 2,2′-dipyridylamine)

Chih-Chieh Wang,*[a] Cheng-Han Yang,[a] and Gene-Hsiang Lee[b]

Keywords: Hydrothermal synthesis / Self-assembly / Hydrogen bonds / Squarate / Cadmium

Two extended coordination frameworks of Cd^{II}–squarate complexes with the formulas $[Cd_2(C_4O_4)_{2.5}(H_2O)_4](dpaH)\cdot 1.5(H_2O)$ (**1**) and $[Cd(C_4O_4)(dpa)(H_2O)]$ (**2**) (dpa = 2,2′-dipyridylamine) have been synthesized under hydrothermal conditions and characterized by single-crystal X-ray diffraction studies. Structural determination reveals that compound **1** consists of a free monoprotonated 2,2′-dipyridylamine ion ($dpaH^+$) and a two-dimensional (2D) anionic, layered framework, $\{[Cd_2(C_4O_4)_{2.5}(H_2O)_4]^-\}$, which is formed with two antiprismatic square-boxes as the fundamental building unit through the connection between Cd^{II} ions and hybrid $\mu_{1,2,3}$-, $\mu_{1,2,3,4}$-squarates. Each square-box acts as a host for the inclusion of one pyridine ring of $dpaH^+$. Adjacent $dpaH^+$ cations are then self-assembled by the parallel alignment of the other pyridine ring of $dpaH^+$ to complete a 3D network with one-dimensional (1D) channels intercalated by water molecules. Compound **2** contains a distorted octahedral Cd^{II} center coordinated by two squarates, two waters and one dpa ligand to form a 1D 2-legged, ladder-like framework by the connection of a $[Cd(dpa)(\mu_2\text{-}H_2O)]_2^{4+}$ dimeric unit and a $\mu_{1,2}$-squarate. Weak π–π stacking interaction and hydrogen bonds of N–H···O, O–H···O and C–H···O among the squarate, water and dpa ligands provide additional intra- and intermolecular interactions on the stabilization of these two polymeric frameworks.

Introduction

Metal-organic frameworks (MOFs)[1–5] have been attracting much attention owing to their potential applications as functional solid materials in gas storage, molecular sieves, size- or shape-selective catalysis, and ion exchange,[6–9] as well as because of their versatile structural topology. The design and synthesis of new open-framework coordination polymers have been the focus in current chemical and new material research. Of particular importance is the ability of the organic molecules to influence profoundly the structures of synthesized products, and to direct their formation with specific structures and potential applications, such as magnetism, host–guest chemistry, shape specificity and catalysis. In a relevant approach, the squarate (dianion of 3,4-dihydroxycyclobut-3-ene-1,2-dione, $H_2C_4O_4$) serves as a unique ligand, which possesses a four-membered cyclic aromatic structure, characterized by extensive π-electron delocalization over all carbon and oxygen atoms. Accordingly, squarate has been known as a polyfunctional ligand providing hydrogen bonding, π–π interactions, and the construction of extended frameworks. It is also widely used as a bridging ligand bonded with metal ions in various bridging modes to create numerous amazing metal–squarate frameworks, including one-dimensional (1D) chain, two-dimensional (2D) layer, three-dimensional (3D) cube- and cage-like frameworks.[10–17] Many squarate-bridged metal complexes with $\mu_{1,2}$- or $\mu_{1,3}$-bridging modes incorporating different nitrogen-based, flexible ligands have been structurally characterized[18–24] and showed interesting magnetic behavior.[25] In this contribution, we report the hydrothermal syntheses, structures and thermal stability of two novel Cd–squarate coordination frameworks, $[Cd_2(C_4O_4)_{2.5}(H_2O)_4](dpaH)\cdot 1.5(H_2O)$ (**1**) and $[Cd(C_4O_4)(dpa)(H_2O)]$ (**2**) by using flexible dpa and rigid squarate ligands as building blocks to form 3D microporous and 1D ladder-like extended networks.

Results and Discussion

Synthesis and IR Spectroscopy of Compounds 1 and 2

The reaction was carried out under hydrothermal conditions, by adjusting various molar ratios of $[Cd(NO_3)_2]\cdot 4H_2O$, dpa and $H_2C_4O_4$ (Table 1). The results showed that compounds **1** and **2** are not controlled by stoichiometry but rather by the pH-controlled products. Compound **1** was the favored product with relatively lower pH value (pH < 4), whereas compound **2** was the dominant product with rela-

---

[a] Department of Chemistry, Soochow University,
111, Taipei, Taiwan
Fax: +886-2-28811053
E-mail: ccwang@mail.scu.edu.tw
[b] Instrumentation Center, National Taiwan University,
Taipei, Taiwan

tively higher pH value (pH > 4). Both compounds are air-stable at ambient temperature and insoluble in common solvents, such as water, alcohol and acetonitrile. The N–H stretching vibrations of both compounds appear in the 3000–3400 cm^{-1} region, and their frequencies are consistent with the existence of hydrogen bonds between N–H and several H-acceptor groups. The most relevant IR features are those associated with the chelating squarate ligands. The coordinated CO groups are characterized by medium absorptions at 1664 and 1656 cm^{-1} for **1** and **2**, respectively. A very strong band centered at around 1500 cm^{-1} is attributed to the vibrational modes of a combination of C–O and C–C stretching motions; the assignment of which is in agreement with the characteristic of the $(CO)_n^{2-}$ salts.[26]

Table 1. Products for different reaction conditions by adjusting molar ratios of $[Cd(NO_3)_2]·4H_2O$, dpa and $H_2C_2O_4$.

Molar ratios in 6 mL water $[Cd(NO_3)_2]·4H_2O$	dpa	$H_2C_4O_4$	pH value	Product
0.1 mmol	0.1 mmol	0.1 mmol	2.45	**1**
0.1 mmol	0.15 mmol	0.1 mmol	3.17	**1**
0.1 mmol	0.2 mmol	0.1 mmol	4.31	**2**
0.1 mmol	0.125 mmol	0.06 mmol	4.13	**2**

Crystal Structure of $[Cd_2(C_4O_4)_{2.5}(H_2O)_4](dpaH)·1.5(H_2O)$ (1)

The X-ray structure determination reveals that compound **1** consists of a 2D anionic $[Cd_2(C_4O_4)_{2.5}(H_2O)_4]^-$ layered MOF [Figure 1 (top)], a monoprotonated dpaH$^+$ [Figure 1 (bottom)], and crystallization water molecules. The 2D anionic $[Cd_2(C_4O_4)_{2.5}(H_2O)_4]^-$ layer consists of three independent slightly distorted octahedral Cd^{II} ions in the asymmetric unit, in which the Cd(1) atom is bonded to six oxygen atoms from four $\mu_{1,2,3}$-squarate and two water molecules with the following bond lengths: Cd(1)–O(1) 2.336(2), Cd(1)–O(3) 2.298(2), Cd(1)–O(5) 2.307(2), Cd(1)–O(7) 2.295(2), Cd(1)–O(11) 2.255(2), and Cd(1)–O(12) 2.234(2) Å (Figure 1). The Cd(2) and Cd(3) atoms are both located at the inversion center [(1.5 2.0 0.0) for Cd(2) and (1.0 1.5 0.0) for Cd(3)] and bonded to six oxygen atoms from two $\mu_{1,2,3}$-squarate, two $\mu_{1,2,3,4}$-squarate and two water molecules with the following bond lengths: Cd(2)–O(2) 2.265(2), Cd(2)–O(9) 2.322(2), Cd(2)–O(13) 2.231(2) and Cd(3)–O(6) 2.318(2), Cd(3)–O(10) 2.279(2), and Cd(3)–O(14) 2.236(2) Å (Figure 1). The corresponding bond lengths of the Cd–O$_{sq}$ and Cd–O$_w$ bonds (Table 2) all fall in the same range analogous to those in the $[Cd(C_4O_4)(H_2O)_2]$ complex.[10] It is important to note that the squarate ligand $(C_4O_4^{2-})$, acting as a bridging ligand with two different bridging modes, plays a key role in the construction of a novel 2D anionic framework. Three crystallographically distinct squarate ligands are found: the first one (C1–C4) adopts a $\mu_{1,2,3}$-bridging mode[12] (Figure 2) to link Cd(1) with Cd(2) (5.926 and 6.065 Å) and Cd(1) with Cd(1) (8.457 Å), respectively. The second one (C5–C8) also adopts a $\mu_{1,2,3}$-bridging mode[12] to link Cd(1) with Cd(3) (5.918

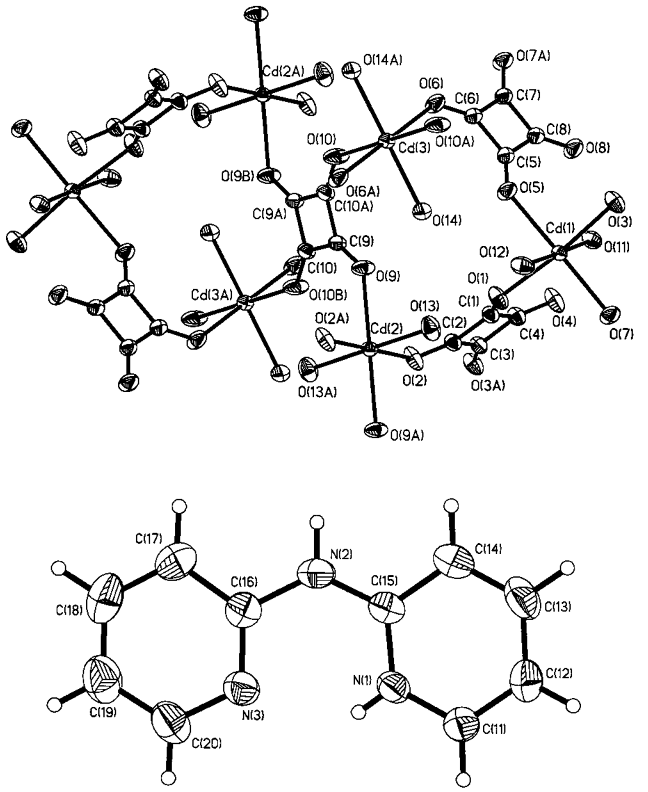

Figure 1. (top) Distorted octahedral coordination spheres of Cd(1), Cd(2) and Cd(3) ions in compound **1** with atom labelling scheme; hydrogen atoms are omitted for clarity. (bottom) Molecular structure of protonated 2,2′-dipyridylamine (dpaH$^+$) cation with atom labelling scheme; dashed lines represent N···H–N hydrogen bond interaction. (ORTEP drawing, thermal ellipsoids at 50% probability level).

Table 2. Selected bond lengths [Å] and angles [°] for compound **1**.[a]

Cd(1)–O(1)	2.336(2)	Cd(1)–O(3)	2.298(2)
Cd(1)–O(5)	2.307(2)	Cd(1)–O(7)	2.295(2)
Cd(1)–O(11)	2.255(2)	Cd(1)–O(12)	2.234(2)
O(1)–Cd(1)–O(3)	174.38(8)	O(1)–Cd(1)–O(5)	84.68(9)
O(1)–Cd(1)–O(7)	94.51(9)	O(1)–Cd(1)–O(11)	93.36(8)
O(1)–Cd(1)–O(12)	83.56(8)	O(3)–Cd(1)–O(5)	89.71(9)
O(3)–Cd(1)–O(7)	91.10(9)	O(3)–Cd(1)–O(11)	86.59(8)
O(3)–Cd(1)–O(12)	92.26(8)	O(5)–Cd(1)–O(7)	178.56(8)
O(5)–Cd(1)–O(11)	93.34(8)	O(5)–Cd(1)–O(12)	84.17(8)
O(7)–Cd(1)–O(11)	87.88(8)	O(7)–Cd(1)–O(12)	94.57(9)
O(11)–Cd(1)–O(12)	176.19(9)	O(2)–Cd(2)–O(2)$_i$	180.0
Cd(2)–O(2) × 2	2.265(2)	Cd(2)–O(9) × 2	2.322(2)
Cd(2)–O(13) × 2	2.231(2)		
O(2)–Cd(2)–O(2)$_i$	180.0	O(2)–Cd(2)–O(9)$_i$	85.85(9)
O(2)–Cd(2)–O(9)	94.15(9)	O(2)–Cd(2)–O(13)$_i$	86.16(9)
O(2)–Cd(2)–O(13)	93.84(9)	O(9)–Cd(2)–O(13)	81.87(9)
O(9)–Cd(2)–O(9)$_i$	180.0	O(13)–Cd(2)–O(13)$_i$	180.0
O(9)–Cd(2)–O(13)$_i$	98.13(9)		
Cd(3)–O(6) × 2	2.318(2)	Cd(3)–O(10) × 2	2.279(2)
Cd(3)–O(14) × 2	2.236(2)		
O(6)–Cd(3)–O(6)$_{ii}$	180.0	O(6)–Cd(3)–O(10)	88.3(1)
O(6)–Cd(3)–O(10)$_{ii}$	91.7(1)	O(6)–Cd(3)–O(14)	97.58(9)
O(6)–Cd(3)–O(14)$_{ii}$	82.42(9)	O(10)–Cd(3)–O(10)$_{ii}$	180.0
O(10)–Cd(3)–O(14)	95.28(9)	O(10)–Cd(3)–O(14)$_{ii}$	84.72(9)
O(14)–Cd(3)–O(14)$_{ii}$	180.0		

[a] Symmetry codes: (i) $-x + 3, -y + 4, -z$; (ii) $-x + 2, -y + 3, -z$.

and 6.057 Å) and Cd(1) with Cd(1) (8.434 Å), respectively. The last one (C9–C10) adopts a $\mu_{1,2,3,4}$-bridging mode[10] (Figure 2) to link Cd(2) with Cd(3) (2 × 5.854 and 2 × 6.088 Å), Cd(2) with Cd(2) (8.434 Å) and Cd(3)···Cd(3) (8.457 Å), respectively. To the best of our knowledge, compound **1** is the first coordination framework consisting of a Cd/squarate system with hybrid $\mu_{1,2,3}$- and $\mu_{1,2,3,4}$-bridging modes of squarates. It is also noted that, independent of $\mu_{1,2,3}$- or $\mu_{1,2,3,4}$-squarates, the differences among the four C–O distances are not obvious, with the averaged C–O distances of 1.254(4) and 1.255(4) Å for $\mu_{1,2,3}$-squarate and 1.252(4) Å for $\mu_{1,2,3,4}$-squarate, respectively. The result indicates a more π-delocalization bridging mode (D_{4h}) close to a free squarate ring. The free, monoprotonated dpaH$^+$ cation shown in Figure 1 (bottom) adopts an *anti-anti* conformation mode. The presence of the proton H(1) bound to N(1) [0.754 Å H(1)–N(1)] and its hydrogen bond with N(3) [2.672(5) Å N(1)···N(3)] accounts for the *anti-anti* conformation of dpaH$^+$ and the quasi co-planarity of the two pyridyl rings [the dihedral angles between the mean planes of two pyridine rings is only 5.22°]. All C–C and C–N bond lengths and bond angles in the dpaH$^+$ molecule are comparable to those reported previously.[27]

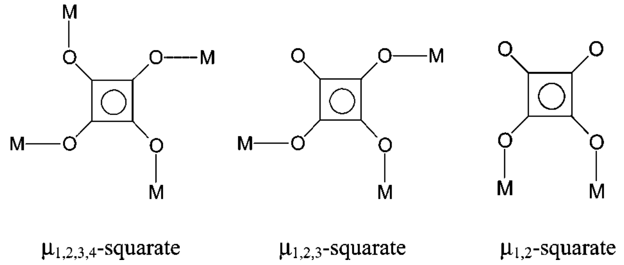

Figure 2. Binding modes of squarate in compound **1** and **2**.

The overall 3D architecture is depicted in Figure 3, and can be described as the self-assembly of 2D anionic Cd–squarate frameworks and free dpaH$^+$ cations. A face-sharing double-box shown in Figure 4 (top) is the fundamental building unit for the construction of the 2D anionic MOF. Each box consists of an antiprismatic square Cd_8 skeleton, bridged by four $\mu_{1,2,3}$-bridge squarates, acting as four sides of the box, and by one $\mu_{1,2,3,4}$-squarate ligand, acting as the base. Two boxes share a $\mu_{1,2,3,4}$-squarate to form a face-sharing double-box unit, whereas the neighboring double-box units share a $\mu_{1,2,3}$-squarate to complete a 2D-extended framework along the [100] and [010] directions. The dimensions of the box are approximately 5.0 × 5.0 × 4.9 Å (shortest oxygen–oxygen contact distances not including the van der Waals radii), providing a vacant space for the inclusion of a pyridyl group of the dpaH$^+$ cation. It is worthy to note that the dpaH$^+$ cation plays the other important role in the construction of this 3D network. It acts not only as a counterion to balance the charge of the Cd–squarate anionic skeleton, but also as an inclusion molecule with one of the pyridyl groups in dpaH$^+$ cation inserting into each antiprismatic box. The pyridyl groups outside the boxes are then aligned parallel to one another (the separation distance of 4.2 Å between two centroid pyridyl groups) to complete the 3D-extended network, which allows a 1D microporous channel along the *c* axis (Figure 2). Two free, disordered water molecules, O15 with 0.5 occupancy and O16, O16′ with 0.67 and 0.33 occupancy, respectively, are intercalated into these channels. Hydrogen-bond formation serves as a important factor and is widely used in constructing coordination polymers.[28–32] In compound **1**, hydrogen-bonding

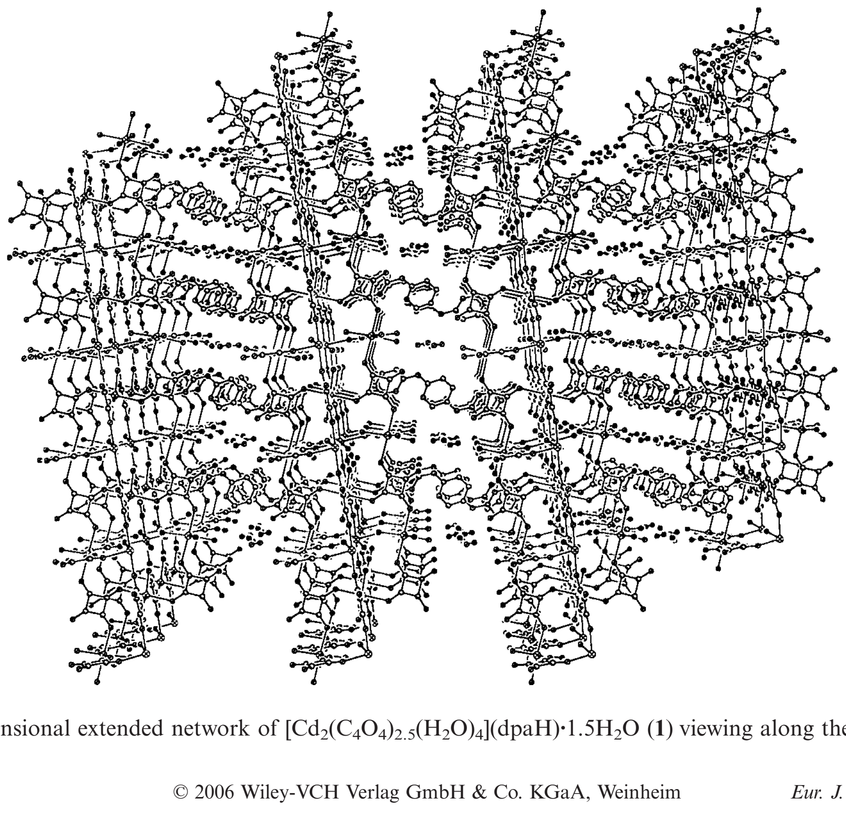

Figure 3. The three-dimensional extended network of $[Cd_2(C_4O_4)_{2.5}(H_2O)_4](dpaH)\cdot 1.5H_2O$ (**1**) viewing along the *a*-axis.

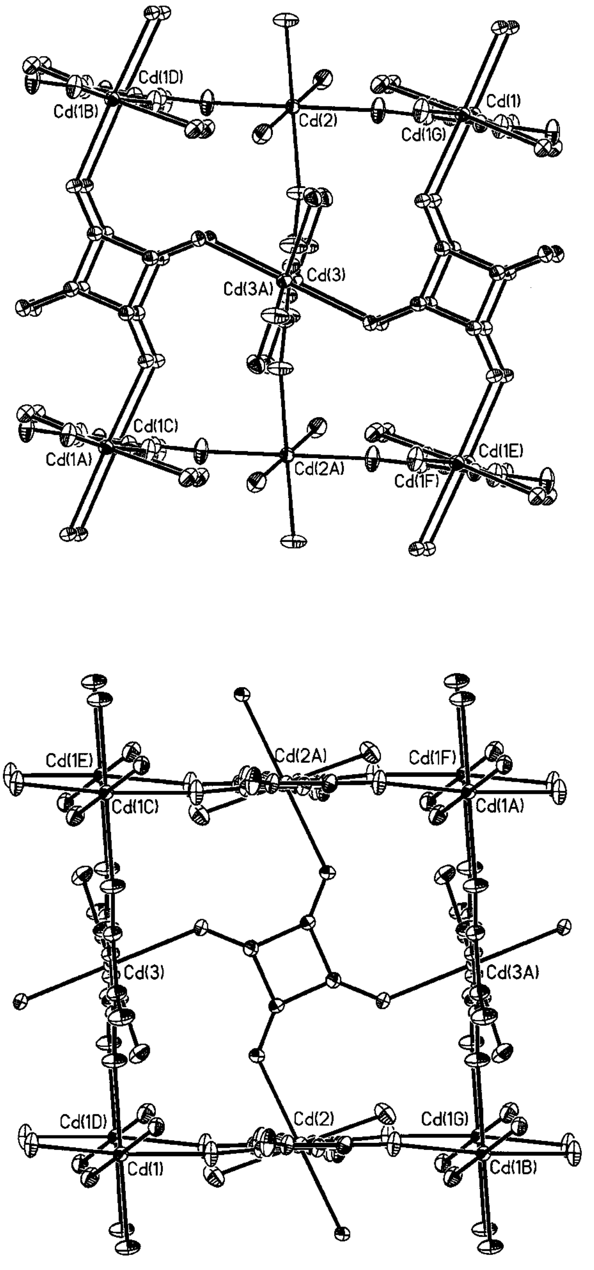

Figure 4. (top) Perspective side view (left) of double-box building unit and (bottom) top view of the *anti*-prism square box in **1**.

interactions, including the N–H···N, N–H···O and O–H···O hydrogen bonds among the dpaH$^+$, squarate ligands and water molecules, provide the additional stabilizing forces to enhance the 3D microporous network. Related bond lengths and angles of the N–H···N, N–H···O and O–H···O hydrogen bonds are summarized in Table 3.

Crystal Structures of [Cd(C_4O_4)(dpa)(H_2O)] (2)

The X-ray structural determination of compound **2** evidences a polymeric arrangement with a linear 2-legged, ladder-like MOF, which is isostructural with [M(C_4O_4)(dpa)(H_2O)], M = Co, Ni, Zn.[33] The Cd^{II} center is six-coordinate and adopts a slightly distorted octahedral coordination environment bonded to two nitrogen atoms from dpa ligands and two oxygen atoms from two squarate ligands and two water molecules. The related bond lengths and bond angles around the Cd center are listed in Table 4. Two Cd ions are linked together through two bridging water molecules to form a [Cd(dpa)(H_2O)]$_2^{4+}$ dimeric fragment (see Figure 5) in the equatorial plane [Figure 5 (top)] with bond lengths of Cd(1)–O(5) 2.330(2), Cd(1)–O(5)$_i$ 2.384(2), Cd(1)–N(1) 2.296(2) and Cd(3)–N(3) 2.276(2) Å. The squarate ligand adopts a $\mu_{1,2}$-binding mode[33] (Figure 2) to connect the neighboring [Cd(dpa)(μ_2-OH_2)]$_2$ fragments at the axial sites with bond lengths of Cd(1)–O(1) 2.240(2), Cd(1)–O(2) 2.269(2) Å, constructing a 1D, linear, 2-legged, ladderlike MOF along the *a* axis [Figure 5 (bottom)]. The corresponding bond lengths of the Cd–O$_{sq}$ and Cd–O$_w$

Table 4. Selected bond lengths [Å] and angles [°] for compound **2**.[a]

Cd(1)–O(1)	2.240(2)	Cd(1)–O(2)	2.269(2)
Cd(1)–O(5)	2.330(2)	Cd(1)–O(5)$_i$	2.384(2)
Cd(1)–N(1)	2.296(2)	Cd(1)–N(3)	2.276(2)
O(1)–Cd(1)–O(2)	176.56(7)	O(1)–Cd(1)–O(5)	90.54(8)
O(1)–Cd(1)–O(5)$_i$	89.12(8)	O(1)–Cd(1)–N(1)	91.83(8)
O(1)–Cd(1)–N(3)	92.20(8)	O(2)–Cd(1)–O(5)	88.05(8)
O(2)–Cd(1)–O(5)$_i$	87.52(8)	O(2)–Cd(1)–N(1)	91.54(8)
O(2)–Cd(1)–N(3)	88.83(8)	O(5)–Cd(1)–O(5)$_i$	77.78(9)
O(5)–Cd(1)–N(1)	103.05(8)	O(5)–Cd(1)–N(3)	172.63(8)
O(5)$_i$–Cd(1)–N(1)	178.73(8)	O(5)$_i$–Cd(1)–N(3)	95.42(8)
N(1)–Cd(1)–N(3)	83.70(9)		

[a] Symmetry code: (i) –*x*, –*y*, –*z*.

Table 3. Hydrogen bond lengths [Å] and angles [°] for compound **1**.[a]

Donor–H		Donor···Acceptor		H···Acceptor		Donor–H···Acceptor	
N(1)–H(1a)	0.754	N(1)···N(3)	2.672(5)	H(1a)···N(3)	2.085	N(1)–H(1a)···N(3)	135.0
N(2)–H(2a)	0.860	N(2)···O(15)	2.951(3)	H(2a)···O(15)	2.143	N(2)–H(2a)···O(15)	156.5
N(2)–H(2a)	0.860	N(2)···O(15)$_i$	2.896(3)	H(2a)···O(15)$_i$	2.036	N(2)–H(2a)···O(15)$_i$	178.00
O(11)–H(11)	0.888	O(11)···O(4)	2.628(3)	H(11)···O(4)	1.741	O(11)–H(11)···O(4)	176.2
O(11)–H(11′)	0.895	O(11)···O(8)$_{ii}$	2.687(3)	H(11′)···O(8)$_{ii}$	1.811	O(11)–H(11′)···O(8)$_{ii}$	165.5
O(12)–H(12)	0.871	O(12)···O(6)$_{iii}$	2.754(3)	H(12)···O(6)$_{iii}$	1.903	O(12)–H(12)···O(6)$_{iii}$	165.4
O(12)–H(12′)	0.890	O(12)···O(2)$_{ii}$	2.732(3)	H(12′)···O(2)$_{ii}$	1.849	O(12)–H(12′)···O(2)$_{ii}$	171.0
O(13)–H(13)	0.873	O(13)···O(1)	2.744(3)	H(13)···O(1)	1.901	O(13)–H(13)···O(1)	162.7
O(13)–H(13′)	0.867	O(13)···O(10)$_{iv}$	2.814(3)	H(13′)···O(10)$_{iv}$	2.016	O(13)–H(13′)···O(10)$_{iv}$	152.6
O(14)–H(14)	0.902	O(14)···O(5)	2.731(3)	H(14)···O(5)	1.849	O(14)–H(14)···O(5)	165.1
O(14)–H(14′)	0.864	O(14)···O(9)$_v$	2.802(3)	H(14′)···O(9)$_v$	1.973	O(14)–H(14′)···O(9)$_v$	160.5

[a] Symmetry codes: (i) –*x*, 1 – *y*, 1 – *z*; (ii) *x*, –1 + *y*, *z*; (iii) 1 + *x*, –1 + *y*, *z*; (iv) 1 – *x*, –*y*, –*z*; (v) *x*, 1 + *y*, *z*; (vi) *x*, 2 + *y*, *z*; (vii) 1 – *x*, 1 – *y*, 1 – *z*; (viii) –1 + *x*, *y*, *z*.

bonds fall in the same range, analogous to those in the $[Cd(C_4O_4)(H_2O)_2]$ complex.[10] The Cd···Cd separations along the μ_2-O_{water} and $\mu_{1,2}$-$C_4O_4^{2-}$ bridges are 3.670(1) and 7.672(1) Å, respectively. It should be noted that adjacent ladders are displaced by half a repeating unit along the *a* and *c* axes. This arrangement effectively prevents steric hindrance between the inter-ladder dpa ligands. As a result, compound **2** favor a closer-packing building block as shown in Figure 6. The centroid pyridine rings in dpa ligands among the adjacent ladders are generally parallel and adopt a face-to-face alignment (Figure 5) with the separation distance of 3.9 Å, indicating a very weak but significant π–π stacking interaction[33–35] that may, in part, contribute to the stabilization of the extended framework. In compound **2**, two strong O–H···O hydrogen bonds [O(5)–H(5a)···O(4) and O(5)–H(5b)···O(3)] are found between uncoordinated oxygen atoms of squarate and the coordinated water molecules with the O···O distances in the range of 2.528–2.600 Å. In addition, the inter-ladder interactions are through one pair of the N–H···O [N(2)–H(2a)···O(4)] and C–H···O [C(11)–H(11a)···O(4)] hydrogen bonds from the same dpa molecule linked to the oxygen atom of squarate in the neighboring ladders to form a mixed N–H···O and C–H···O hydrogen bonds (dashed line in Figure 6). Similar hydrogen-bonding interactions have also been found in the

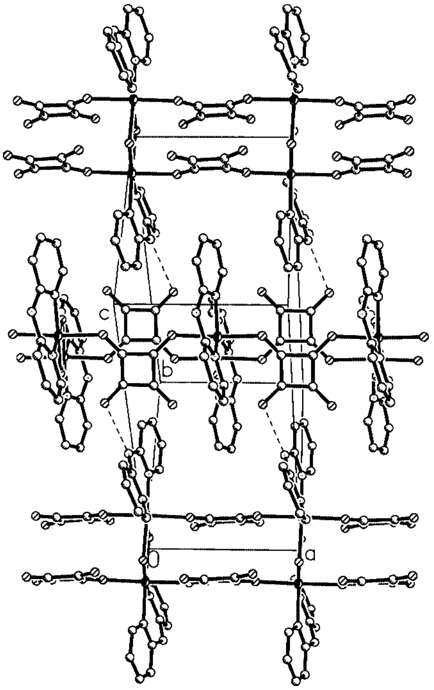

Figure 6. The molecular packing of the ladder-like framework in **2**; dashed lines represent H-bond interactions.

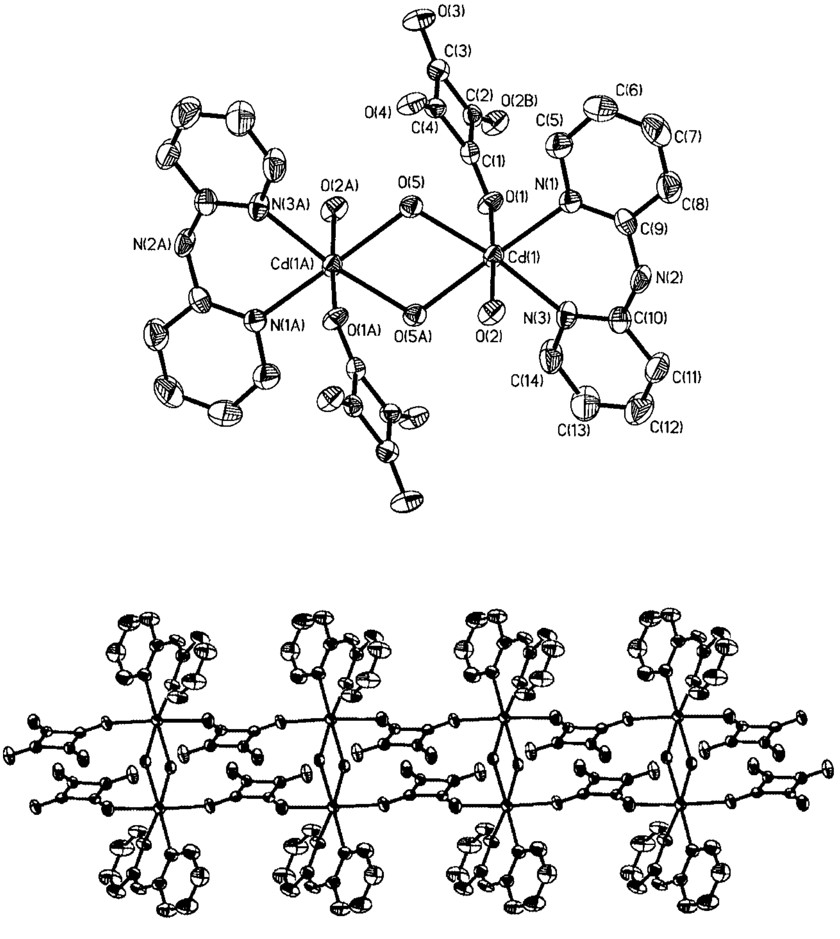

Figure 5. (top) Molecular structure of compound **2** with atom labelling scheme; hydrogen atoms are omitted for clarity. (ORTEP drawing, thermal ellipsoids at 50% probability level) (bottom) Perspective view of a 2-legged, ladder-like framework along the *a* axis in **2**.

Table 5. Hydrogen bond lengths [Å] and angles [°] for compound **2**.[a]

Donor–H [Å]		Donor···Acceptor [Å]		H···Acceptor [Å]		Donor–H···Acceptor [°]	
O(5)–H(5a)	0.735	O(5)···O(4)	2.600(3)	H(5a)···O(4)	1.883	O(5)–H(5a)···O(4)	163.1
O(5)–H(5b)	0.922	O(5)···O(3)$_i$	2.590(3)	H(5b)···O(3)$_i$	1.672	O(5)–H(5b)···O(3)$_i$	174.0
N(2)–H(2a)	0.860	N(2)···O(4)$_{ii}$	2.890(3)	H(2a)···O(4)$_{ii}$	2.092	N(2)–H(2a)···O(4)$_{ii}$	154.1
C(11)–H(11a)	0.930	C(11)···O(4)$_{ii}$	3.204(4)	H(11a)···O(4)$_{ii}$	2.430	C(11)–H(11a)···O(4)$_{ii}$	140.6

[a] Symmetry codes: (i) –1 + *x*, *y*, *z*; (ii) 0.5 + *x*, 0.5 – *y*, 0.5 + *z*.

[Fe(oxa)(dpa)][28] (oxa = oxalate) and [M_2(dpa)$_2$(C_2O_4)(C_4O_4)] (M = Cu, Zn) complexes.[34] Related bond lengths and angles of the O–H···O, N–H···O and C–H···O hydrogen bonds for **2** are summarized in Table 5.

Thermogravimetric Analysis

To investigate the thermal stability of the 3D and 1D extended framework of **1** and **2**, the thermogravimetric analyses (TGA) were performed on samples consisting of numerous single crystals under nitrogen. The TGA data of **1** suggest that the first weight lost of 11.24% (calcd. 12.75%), corresponding to the lost of 1.5 solvated and four coordinated water molecules at the cadmium center, occurred over the range of 30–174 °C. In the temperature range of 180–312 °C, **1** underwent the weight lost of 24.64% corresponding to the lost of dpaH$^+$ cations (calcd. 22.16%). The resulting solid then slowly decomposed with loss of squarate ligands to yield cadmium oxide (CdO). Compound **2** underwent a continuous single-step weight-loss process (losing coordinated water first, and then dpa and squarate groups). The on-set temperature of the weight loss is approximately at 201 °C. The decomposition process was completed at approximately 391 °C and the final product of the pyrolysis is CdO.

Conclusion

In conclusion, under hydrothermal conditions, we have successfully synthesized two pH-controlled Cadmium(II)–squarate compounds, [$Cd_2(C_4O_4)_{2.5}(H_2O)_4$](dpaH)·1.5($H_2O$) (**1**) and [Cd($C_4O_4$)(dpa)($H_2O$)] (**2**), with metal-organic frameworks; the structures of which are well characterized by X-ray diffraction method. In compound **1**, the overall 3D network with 1D microporous channels is constructed by the following intra- and inter-molecular interactions: (1) metal–squarate covalent bonds to form a anionic 2D framework through the connectivity between Cd ions and hybrid $\mu_{1,2,3}$- and $\mu_{1,2,3,4}$-squarates, (2) molecular inclusion of dpaH$^+$ pyridyl group into the antiprism square box, (3) π–π stacking interaction of pyridyl groups between neighboring dpaH$^+$ cations and (4) hydrogen bonds between water molecules, squarate and dpaH$^+$. For compound **2**, the squarate ligands afford a $\mu_{1,2}$-bridging coordination mode as well as hydrogen-bonding capability to build a 1D 2-legged, ladder-like MOF.

Experimental Section

Materials and Physical Techniques: All chemicals were of reagent grade and were used as commercially obtained without further purification. Elementary analyses (carbon, hydrogen and nitrogen) were performed using a Perkin–Elmer 2400 elemental analyzer. IR spectra were recorded with a Nicolet Fourier Transform IR, MAGNA-IR 500 spectrometer in the range of 500–4000 cm^{-1} using the KBr disc technique. Thermogravimetric analyses (TGA) of compounds **1** and **2** were performed with a computer-controlled Perkin–Elmer 7 Series/UNIX TGA7 analyzer. Single-phased powder samples of **1** (4.014 mg) and **2** (1.228 mg) were loaded into alumina pans and heated with a ramp rate of 5 °C/min from room temperature to 900 °C under nitrogen.

Synthesis of [$Cd_2(C_4O_4)_{2.5}(H_2O)_4$](dpaH)·1.5$H_2O$ (1): The reaction of Cd(NO_3)$_2$·4H_2O (0.0325 g, 0.1 mmol), dpa (0.0175 g, 0.1 mmol), $H_2C_4O_4$ (0.0118 g, 0.1 mmol), and deionized water (6 mL, 0.3333 mol) in the molar ratio 1:1:1:3.333, in a Teflon-lined acid digestion bomb at 180 °C for three days, followed by slow cooling at 6 °C/h to room temperature, yielded colorless solutions. After evaporation for several days at room temperature, colorless crystals grew out of solution as needles and were collected after filtration and drying (yield: 0.0106 g, 34%). The final pH value was 2.45. $C_{20}H_{21}Cd_2N_3O_{15.5}$ (776.20): calcd. C 30.95, N 5.41, H 2.73; found C 30.99, N 5.39, H 2.58. IR (4000–400 cm^{-1}): $\tilde{\nu}$ = 3246 (m), 3083 (m), 1664 (m), 1610 (m), 1563 (m), 1506 (vs), 1457 (s), 1246 (w), 777 (m) cm^{-1}.

Synthesis of [Cd(C_4O_4)(dpa)(H_2O)] (2): The compounds Cd(NO_3)$_2$·4H_2O (0.0322 g, 0.1 mmol), dpa (0.0351 g, 0.2 mmol), $H_2C_4O_4$ (0.0116 g, 0.1 mmol), and deionized water (6 mL, 0.3333 mol) in the mol ratio 1:2:1:3.333 were sealed in a Teflon-lined acid digestion bomb at 180 °C for three days. They were then cooled at 6 °C/h to room temperature, yielding colorless plate crystals after filtration and drying (0.0162 g, 39%). The final pH value was 4.31. $C_{14}H_{11}CdN_3O_5$ (413.66): calcd. C 40.65, H 2.68, N 10.16; found C 40.31, H 2.81, N 10.34. IR (4000–400 cm^{-1}): $\tilde{\nu}$ = 3320 (w), 3206 (m), 3138 (m), 3082 (m), 3045 (m), 1656 (m), 1599 (m), 1538 (s), 1504 (vs), 1474 (vs), 1428 (s), 1373 (m), 1232 (m), 763 (m) cm^{-1}.

X-ray Crystallographic Study: Crystallographic data and experimental details of refinements for structural analyses are given in Table 6. Data collections of **1** and **2** were carried out with a Siemens SMART diffractometer with a CCD detector with Mo radiation (λ = 0.71073 Å) at room temperature. A preliminary orientation matrix and unit cell parameters were determined from 3 runs of 15 frames each, each frame correspond to a 0.3°scan in 10 s, following by spot integration and least-squares refinement. For each structure, data were measured using ω scans of 0.3° per frame for 20 s until a complete hemisphere had been collected. Cell parameters were retrieved with SMART[36] software and refined with SAINT[37] on all observed reflections. Data reduction was performed with the SAINT[37] software and corrected for Lorentz and polarization effects. Absorption corrections were applied with the program SADABS.[38] Direct phase determination and subsequent difference Fourier map synthesis yielded the positions of all non-hydrogen atoms, which were subjected to anisotropic refinements. All hydrogen atoms were generated geometrically (C–H: 0.95) with the exception of the hydrogen atoms of the coordinated water molecules, which were located in the difference Fourier map with the corresponding positions and isotropic displacement parameters being refined. The final full-matrix, least-squares refinement on F^2 was applied for all observed reflections [$I > 2\sigma(I)$]. All calculations were performed by using the SHELXTL software package.[39]

Table 6. Crystal data for compounds **1** and **2**.

	1	**2**
Empirical formula	$C_{20}H_{21}Cd_2N_3O_{15.50}$	$C_{14}H_{11}CdN_3O_5$
Molecular weight	776.20	413.66
Crystal system	triclinic	monoclinic
Space group	$P\bar{1}$	$P2_1/n$
a [Å]	8.4341(2)	7.6720(3)
b [Å]	8.4570(2)	11.1502(4)
c [Å]	18.0891(4)	16.8908(6)
α [°]	81.0679(4)	
β [°]	88.2877(4)	91.267(1)
γ [°]	87.7564(4)	
V [Å^3]	1273.25(5)	1444.56(9)
Z	2	4
$D_{calcd.}$ [g cm^{-3}]	2.025	1.902
T [K]	295(2)	295(2)
μ [mm^{-1}]	1.754	1.542
Reflections collected	17890	12538
Reflections unique / R_{int}	5828 / 0.033	3319 / 0.040
Reflections with [$I > 2\sigma(I)$]	4627	2378
N_v	395	216
R_F[a], R_w[b] (all data)	0.0371, 0.0676	0.0543, 0.0523
R_F[a], R_w[b] [$I > 2\sigma(I)$]	0.0243, 0.0540	0.0289, 0.0495
Goodness-of-fit	1.006	1.010
$\Delta\rho_{max.}$ / $_{min.}$ [e Å^3]	+0.79 / –0.56	+0.40 / –0.35

[a] $R_F = \Sigma||F_o| - |F_c||/\Sigma|F_o|$. [b] $R_w(|F|^2) = [\Sigma w(|F_o|^2 - |F_c^2|)^2/\Sigma w|F_o|^2]^{1/2}$.

CCDC-196616 (for **1**) and -205775 (for **2**) contain the supplementary crystallographic data for this paper. These data can be obtained free of charge from The Cambridge Crystallographic Data Centre via www.ccdc.cam.ac.uk/data_request/cif.

Acknowledgments

The authors are grateful for financial support from the National Science Council of the Republic of China (R.O.C).

---

[1] B. F. Hoskins, R. Robson, *J. Am. Chem. Soc.* **1990**, *112*, 15461554.

[2] S. R. Batten, R. Robson, *Angew. Chem. Int. Ed.* **1998**, *37*, 1460–1494.

[3] A. N. Khlobystov, A. J. Blake, N. R. Champness, D. A. Lemenovskii, A. G. Majouga, N. V. Zyk, M. Schröder, *Coord. Chem. Rev.* **2001**, *222*, 155–192.

[4] M. Eddaoudi, D. B. Moler, H. L. Li, B. L. Chen, T. M. Reineke, M. O'Keeffe, O. M. Yaghi, *Acc. Chem. Res.* **2001**, *34*, 319–330.

[5] B. Moulton, M. J. Zaworotko, *Chem. Rev.* **2001**, *101*, 1629–1658.

[6] C. Janiak, *Angew. Chem. Int. Ed. Engl.* **1997**, *36*, 1431–1434.

[7] H. Li, M. Eddaoudi, M. O'Keeffe, O. M. Yaghi, *Nature* **1999**, *402*, 276.

[8] S. Noro, R. Kitaura, M. Kondo, S. Kitagawa, T. Ishii, H. Matsuzaka, M. Yamashita, *J. Am. Chem. Soc.* **2002**, *124*, 2568–2583.

[9] C. J. Kepert, M. J. Rosseinsky, *Chem. Commun.* **1998**, 31–32.

[10] C. R. Lee, C. C. Wang, Y. Wang, *Acta Crystallogr. Sect. B* **1996**, *52*, 966–975.

[11] D. S. Yufit, D. J. Price, J. A. K. Howard, S. O. H. Gutschke, A. K. Powell, P. T. Wood, *Chem. Commun.* **1999**, 1561–1562.

[12] K. J. Lin, K. H. Lii, *Angew. Chem. Int. Ed. Engl.* **1997**, *36*, 2076–2077.

[13] J. Spandl, I. Brüdgam, H. Hartl, *Angew. Chem. Int. Ed.* **2001**, *40*, 4018–4020.

[14] H.-A. Hosein, H. Jaggernauth, B. D. Alleyne, L. A. Hall, A. J. P. White, D. J. Williams, *Inorg. Chem.* **1999**, *38*, 3716–3720.

[15] T. K. Maji, G. Mostafa, S. Sain, J. S. Prasad, N. R. Chaudhuri, *Cryst. Eng. Commun.* **2001**, 37.

[16] a) M. I. Khan, Y. D. Chang, Q. Chen, J. Salta, Y. S. Lee, C. J. O'Connor, J. Zubieta, *Inorg. Chem.* **1994**, *33*, 6340–6350; b) A. Müller, R. Rohlfing, E. Krickemeyer, H. Bögge, *Angew. Chem. Int. Ed. Engl.* **1993**, *32*, 909–912.

[17] Q. Chen, S. Liu, J. Zubieta, *Angew. Chem. Int. Ed. Engl.* **1990**, *29*, 70–72.

[18] I. Castro, M. L. Calatayud, J. Sletten, F. Lloret, M. Julve, *J. Chem. Soc. Dalton Trans.* **1997**, 811–818.

[19] R. Soules, F. Dahan, J.-P. Laurent, P. Castan, *J. Chem. Soc. Dalton Trans.* **1988**, 587–590.

[20] J. A. C. van Ooijen, J. Reedijk, A. L. Spek, *Inorg. Chem.* **1979**, *18*, 1184–1189.

[21] C. E. Xanthopoulos, M. P. Sigalas, G. A. Katsoulos, C. A. Tsipis, C. C. Hadjikostas, A. Terzis, M. Mentzafos, *Inorg. Chem.* **1993**, *32*, 3743–3747.

[22] I. Castro, J. Faus, M. Julve, Y. Journaux, J. Sletten, *J. Chem. Soc. Dalton Trans.* **1991**, 2533–2538.

[23] X. Solans, M. Aguiló, A. Gieizes, J. Faus, M. Julve, *Inorg. Chem.* **1990**, *29*, 775–784.

[24] I. Castro, J. Faus, M. Julve, *Inorg. Chim. Acta* **1990**, *170*, 251.

[25] a) P. S. Mukherjee, S. Konar, E. Zangrando, C. Diaz, J. Ribas, N. R. Chaudhuri, *J. Chem. Soc. Dalton Trans.* **2002**, 3471–3476; b) Y. Akhriff, J. Server-Carrió, A. Sancho, J. García-Lozano, E. Escrivá, L. Soto, *Inorg. Chem.* **2001**, *40*, 6832–6840.

[26] M. Ito, R. Weiss, *J. Am. Chem. Soc.* **1963**, *85*, 2580–2584.

[27] R. Lescouëzec, G. Marinescu, M. C. Muñoz, D. Luneau, M. Andruh, F. Lloret, J. Faus, M. Julve, J. A. Mata, R. Llusar, J. Cano, *New J. Chem.* **2001**, *25*, 1224–1235.

[28] a) J. Y. Lu, A. M. Babb, *Inorg. Chim. Acta* **2001**, *318*, 186–190; b) J. Y. Lu, T. J. Schroeder, A. M. Babb, M. Olmstead, *Polyhedron* **2001**, *20*, 2445–2449.

[29] C. Janiak, *J. Chem. Soc. Dalton Trans.* **2000**, 3885–3896.

[30] S. B. Ferguson, E. M. Sanford, E. M. Seward, F. Diederich, *J. Am. Chem. Soc.* **1991**, *113*, 5410–5419.

[31] R. H. Groeneman, L. R. MacGillivray, J. L. Atwood, *Inorg. Chem.* **1999**, *38*, 208–209.

[32] J. Y. Lu, T. Paliwala, S. C. Lim, C. Yu, T. Niu, A. J. Jacobson, *Inorg. Chem.* **1997**, *36*, 923–929.

[33] C. C. Wang, C. H. Yang, G. H. Lee, H. L. Tsai, *Eur. J. Inorg. Chem.* **2005**, 1334–1342.

[34] C. H. Yang, C. M. Chou, G. H. Lee, C. C. Wang, *Inorg. Chem. Commun.* **2003**, *6*, 135–140.

[35] A. J. Blake, S. J. Hill, P. Hubberstey, W. Li, *J. Chem. Soc. Dalton Trans.* **1997**, 913–914.

[36] *SMART Software for CCD Detector System*, Siemens Analytical Instruments Division: Madison, WI, **1997**.

[37] *SAINT Software for CCD Detector System*, Siemens Analytical Instruments Division: Madison, WI, **1997**.

[38] G. M. Sheldrick, *Program for the Refinement of Crystal Structures*, University of Göttingen: Göttingen, Germany, **1997**.

[39] *SHELXTL*, Program Liberary for Structure Solution and Molecular Graphics, Siemens Analytical Instruments Division: Madison, WI, **1997**.

Received: August 23, 2005
Published Online: December 27, 2005